Nucleation and bubble growth in a first-order cosmological electroweak phase transition

K. Enqvist*
Nordita, Blegdamsvej 17, DK 2100 Copenhagen, Denmark

J. Ignatius,† K. Kajantie,‡ and K. Rummukainen§
Department of Theoretical Physics, Siltavuorenpenger 20 C, 00170 Helsinki, Finland
(Received 16 August 1991)

We study the kinetics of first-order cosmological phase transitions assuming a four-parameter form for the Higgs potential driving the transition. This leads to a phenomenological equation of state for electroweak matter with a stable high-T phase for $T > T_c$ and a low-T phase for $T < T_c$. The nucleation probability of low-T bubbles, both critical and subcritical, is computed and their growth and coalescence is simulated. We show that they can grow as deflagrations and that detonations are unlikely. Possible front velocities and entropy production are studied. The results are applied to parameter values conjectured for the electroweak phase transition and compared with those obtained for the quark→hadron phase transition.

PACS number(s): 98.80.Cq

I. INTRODUCTION

Recently it has become increasingly evident that the electroweak phase transition will play a significant role in the generation of the cosmological baryon asymmetry [1,2]. The symmetry breaking and *CP*- and *B*-violating details of the finite-T phase transition are unknown, but it clearly has to be of first order to provide the necessary condition of thermal nonequilibrium. The purpose of this paper is to study the kinetics of this electroweak (EW) phase transition in cosmology.

Nonequilibrium phenomena can only be studied after equilibrium phenomena are under control. In view of this, the first task is to develop a phenomenological equation of state (EOS) for EW matter with the desired properties: a high-T phase h and a low-T phase l separated by a first-order transition at $T = T_c$ and with associated metastable superheated and supercooled branches.

The crucial parameter of the EOS is $B(T)$, the free energy density difference between the two phases. By definition of T_c it satisfies $B(T_c) = 0$. To obtain $B(T)$ we shall use a mean-field expansion of the free energy density of the electroweak system [3]. The mean field is the order parameter ϕ, which may be identified with some linear combination of the Higgs fields, but in principle contains also all the other fields in the electroweak theory. The expansion is valid for T near T_c and depends on four parameters, which, in principle, are to be determined by experiment. By construction they thus are gauge independent.

The quark→hadron phase transition is also assumed to be of first order and the associated cosmological phase transition has been studied in detail [4–7], especially in view of its effects on light element nucleosynthesis [8]. This transition is characterized by the fact that the latent heat is very large, almost equal to the energy density of the high-T quark phase at T_c, and that the number of relativistic active degrees of freedom changes considerably at $T = T_c$. The phenomenological EOS often used in this context is the bag EOS, which in its simplest version corresponds to choosing $B(T) = \frac{1}{4}L(1 - T^4/T_c^4)$, where L = latent heat $= 4B$, B = bag constant. One-loop calculations of $B(T)$, based on certain assumptions of the QCD vacuum, have also been attempted [9–12]. In the EW theory the latent heat $L = -T_c B'(T_c)$ is small, much less than the energy density of the high-T phase at T_c, and the effective number of degrees of freedom g_* is essentially unchanged at T_c. With the $B(T)$ derived from the mean-field expansion our EOS will also apply better the smaller L/g_* is.

The form of the free energy expansion we choose can also be motivated by considering the q-state d-dimensional Potts model [13], which is known to have a first-order phase transition for $q \geq 3$. This is a lattice model in which the spin on each site can have the value $\sigma_i = 0, 1, \ldots, q-1$ and the energy of a link is $-K$ if the spins are the same at the ends of the link, zero otherwise. If x_i (with $\sum x_i = 1$) is the probability of σ_i, we can define an order parameter s, $0 \leq s \leq 1$, by

$$x_0 = \frac{1+(q-1)s}{q}, \quad x_{i\neq 0} = \frac{1-s}{q}, \tag{1.1}$$

so that the system orders itself to the state 0 ($s \to 1$) for $T \to 0$. The mean-field expansion of the free energy per site then becomes

*Electronic address: enqvist@nbivax.nbi.dk.
†Electronic address: ignatius@finuhcb.
‡Electronic address: kajantie@finuhcb.
§Electronic address: rummukai@cernum.

$$f(s)-f(0)=-\frac{q-1}{q}K\,ds^2+\frac{1+(q-1)s}{q}T\ln[1+(q-1)s]+\frac{q-1}{q}(1-s)T\ln(1-s)$$
$$=\frac{q-1}{2q}(qT-2\,dk)s^2-\tfrac{1}{6}T(q-1)(q-2)s^3+\tfrac{1}{12}T(q-1)(q^2-3q+3)s+\cdots\,. \tag{1.2}$$

The crucial term giving rise to a first-order transition is the cubic one, with its negative coefficient $\sim -T$. Our mean-free expansion will contain a similar cubic term.

The parametrization of the effective potential $V(\phi,T)$ and the properties of the free energy-density difference $B(T)$ following from it are discussed in Sec. II. Knowing $B(T)$ permits us to simply write down the EOS for EW matter near $T=T_c$ in a simple form. This EOS can further be approximated by including just the terms linear in $T-T_c$ in $B(T)$. Knowing $V(\phi,T)$ permits one to compute the nucleation probability. We show in Sec. III that, in spite of it depending on four parameters, it can when properly scaled be expressed as a function of one variable only. Our formulation also permits us to discuss a recently presented scenario [14] for first-order phase transitions including subcritical bubbles in rather explicit terms. Section IV discusses how bubbles are nucleated, grow and fill the space. They can grow as deflagrations or detonations and the possible velocities and associated entropy production are discussed in Sec. V.

II. EFFECTIVE POTENTIAL AND THE EQUATION OF STATE

Qualitatively, we expect the equation of state of the electroweak system to be like that shown in Fig. 1. The system can exist in two phases, a symmetric high-T phase with pressure $p_h(T)$ $(=-F/V)$ (h for high) and a low-T phase with broken symmetry and pressure $p_l(T)$ (l for low). At the transition temperature T_c,

$$p_h(T_c)=p_l(T_c)\,,\quad L\equiv T_c[p_h'(T_c)-p_l'(T_c)]>0\,, \tag{2.1}$$

where L is the latent heat and $p'(T)=s(T)$ is the entropy density. For $T_0<T<T_c$ the system can exist in a metastable supercooled symmetric phase and for $T_c<T<T_+$ in a metastable superheated broken-symmetry phase. We shall write down an explicit phenomenological EOS at the end of this section and study first its most essential feature: the difference $B(T)$ of the free energy densities of the two phases and the effective potential leading to this.

A. Expansion of the effective potential

An expansion of the free energy density leading to the above phase structure is, in analogy with Eq. (1.2),

$$V(\phi,T)=\tfrac{1}{2}M^2(T)\phi^2-\tfrac{1}{3}\delta(T)\phi^3+\tfrac{1}{4}\lambda\phi^4$$
$$=\tfrac{1}{2}\gamma(T^2-T_0^2)\phi^2-\tfrac{1}{3}\alpha T\phi^3+\tfrac{1}{4}\lambda\phi^4\,, \tag{2.2}$$

where $\phi\geq 0$ and γ, α, λ, and T_0 are parameters [3]. When $T>T_0$ $V(\phi,T)$ has always one minimum at $\phi=0$, where $V=0$ and the symmetry is unbroken. Note that the form (2.2) of the free energy follows from the usual large T/M expansion ([4] and Eq. (2.27) below) of the free energy of an ideal gas of particles with mass $M\sim\phi$. Here we regard it as a phenomenological expansion with physical and gauge-invariant expansion coefficients, and we shall neglect any possible higher-order terms in the expansion for $V(\phi,T)$. If

$$\lambda M^2(T)=\tfrac{2}{9}\delta^2(T) \tag{2.3}$$

$V(\phi,T)$ can be written in the form

$$\tfrac{1}{4}\lambda\phi^2\left[\phi-\frac{2\delta}{3\lambda}\right]^2 \tag{2.4}$$

and there is a second degenerate minimum. Thus a solution of Eq. (2.3) defines T_c. If $M^2(T)=\gamma(T^2-T_0^2)$ and $\delta(T)=\alpha T$ are as given in (2.2) a solution

$$T_c^2=\frac{T_0^2}{1-\frac{2}{9}\frac{\alpha^2}{\lambda\gamma}} \tag{2.5}$$

exists if

$$\frac{\alpha^2}{\lambda\gamma}<\frac{9}{2}\,. \tag{2.6}$$

We shall later argue that $\alpha^2/\lambda\gamma$ actually should be less

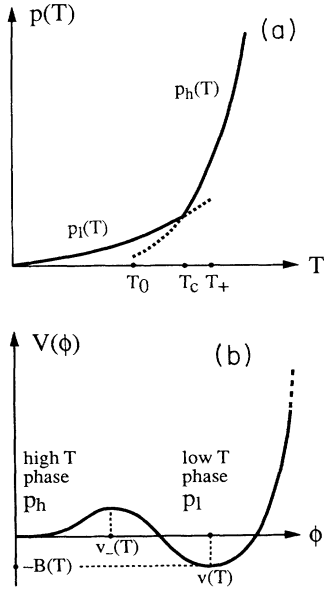

FIG. 1. (a) The equation of state with a first-order phase transition and with two metastable branches; (b) the shape of the effective potential [$v(T)$, $v_-(T)$, and $B(T)$ are given by Eqs. (2.9) and (2.14)].

than about 2. Using Eq. (2.5) one can replace the combination $\alpha^2/\lambda\gamma$ of the parameters by the more physical temperature ratio $\hat{T}_0 \equiv T_0/T_c$ (we shall often denote quantities scaled by T_c by a hat). It will prove convenient to use Eq. (2.3) to define a function

$$\bar{\lambda}(T)=\frac{9}{2}\lambda\frac{M^2(T)}{\delta^2(T)}=\frac{9}{2}\frac{\lambda\gamma}{\alpha^2}\left[1-\frac{T_0^2}{T^2}\right]$$
$$=\frac{1-T_0^2/T^2}{1-T_0^2/T_c^2}=\frac{t_0-t}{t_0-t_c}\ , \qquad (2.7)$$

where the last form holds for cosmological expansion with constant g_*, $tT^2=t_cT_c^2=t_0T_0^2$. The T dependence of the results can often be expressed in terms of the function $\bar{\lambda}(T)$, which satisfies $\bar{\lambda}(T_0)=0$, $\bar{\lambda}(T_c)=1$, $\bar{\lambda}(T_+)=\frac{9}{8}$.

Parenthetically, it is also conceivable that $\delta(T)=\text{const}=\alpha T_s$, where T_s is some fixed temperature scale. Then, independently of T_0,

$$T_c^2=T_s^2\left[1+\frac{2}{9}\frac{\alpha^2}{\lambda\gamma}\right]$$

for all parameter values.

We shall next consider in turn the following quantities of interest derivable from the potential (2.2).

(i) The value $v(T)$ at which the second minimum of the potential occurs. This is the expectation value $\langle\phi\rangle$ of the order parameter ("Higgs field") ϕ.

(ii) The value $-B(T)=V(v(T),T)$ of the potential at this second minimum. This is also the difference between the free energy densities of the two states of the system:

$$p_l(T)-p_h(T)=B(T)\ ,$$
$$s_l(T)-s_h(T)=B'(T)\ . \qquad (2.8)$$

(iii) The correlation lengths in the low-T phase, $l_l=1/\sqrt{V''(v(T),T)}$ and in the high-T phase, $l_h=1/M(T)$.

For $v(T)$ one finds

$$v(T)=\frac{\alpha}{2\lambda}T\left[1+\sqrt{1-\tfrac{8}{9}\bar{\lambda}(T)}\right]\ . \qquad (2.9)$$

The maximum of V (Fig. 1) is at $v_-(T)$, obtained by changing the sign of the square root. Thus a second minimum only exists if $\bar{\lambda}(T)\le\frac{9}{8}$, i.e., for

$$T^2\le T_+^2=\frac{8T_0^2}{9\hat{T}_0^2-1}\ . \qquad (2.10)$$

Above T_+ the superheated metastable low-T phase does not exist. One observes that the parametrization (2.2) does not permit one to fix the physical temperatures T_0, T_c, and T_+ independently. Second, when T_0/T_c decreases, T_+ increases and even goes to infinity when $T_0/T_c=\frac{1}{3}$. It is physically quite unlikely that the metastable superheated l phase could exist at $T\gg T_c$. We thus conclude that the parametrization (2.2) should not be used for too small T_0/T_c, certainly not down to $T_0/T_c=\frac{1}{3}$.

From (2.9) one finds the special values

$$v(0)=\left[\frac{\gamma}{\lambda}\right]^{1/2}T_0=\left[\frac{2}{9(1-\hat{T}_0^2)}\right]^{1/2}\frac{\alpha}{\lambda}T_0\ , \qquad (2.11)$$

$$v(T_0)=\frac{\alpha}{\lambda}T_0\ ,\quad v(T_c)=\frac{2}{3}\frac{\alpha}{\lambda}T_c\ ,\quad v(T_+)=\frac{1}{2}\frac{\alpha}{\lambda}T_+\ , \qquad (2.12)$$

and Fig. 2 shows the full T range. One observes that $v(T)$ always starts increasing from $T=0$ and that it has a maximum at the temperature

$$T_v^2=\frac{9(1-\hat{T}_0^2)}{9\hat{T}_0^2-1}T_0^2=\frac{1}{4\lambda\gamma/\alpha^2-1}\ . \qquad (2.13)$$

For $T_0\lesssim T_c$ the increase stops at small T far below the metastability range and $v(T)$ starts decreasing with increasing T as in Fig. 2. For $T_0/T_c=\sqrt{5/3}$, $T_v=T_0$; decreasing T_0/T_c to 1/3 moves T_v to ∞. For these small values of $\hat{T}_0$, $v(T)$ actually increases practically linearly with T over the metastability range. Again, this is rather unnatural and would imply that the higher-order terms in the expansion (2.2) are important. Hence T_0/T_c should not be too small.

For minus the value of the potential at the second minimum one similarly obtains

$$B(T)=-V(v(T),T)$$
$$=\frac{\alpha^4}{24\lambda^3}T_4\{\tfrac{8}{27}\bar{\lambda}^2(T)-\tfrac{4}{3}\bar{\lambda}(T)+1+[1-\tfrac{8}{9}\bar{\lambda}(T)]^{3/2}\} \qquad (2.14)$$

with the special values

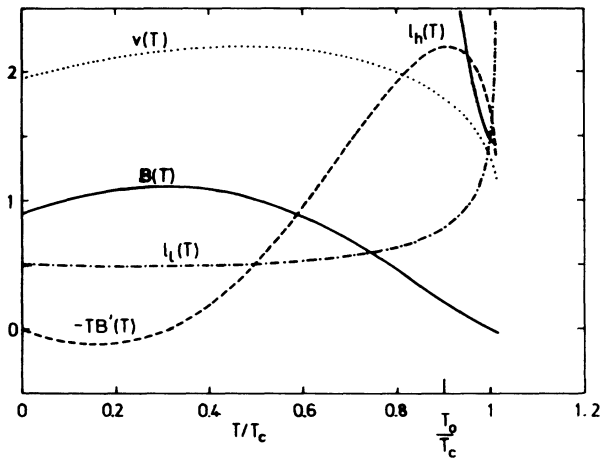

FIG. 2. The functions $v(t)$ [scaled by $\alpha T_c/(2\lambda)$], $B(T)$, $-TB'(T)$ [scaled by $\alpha^4T_c^4/(4\lambda^3)$] and l_l, l_h [scaled by $\sqrt{2\lambda}/(\alpha T_c)$] plotted for $T_0=0.9T_c$, $T_+=1.015T_c$. The curves are plotted for the whole range $0<T<T_+$ although the metastable phase only exists for $T>T_0$.

$$
\begin{aligned}
&B(0)=\frac{\gamma^2}{4\lambda}T_0^4\ ,\quad B(T_b)=\left[\frac{\alpha^2\gamma}{4\lambda^2}\right]^2 T_c^4\ ,\\
&T_b^2=\tfrac{1}{2}(T_c^2-T_0^2)\ ,\\
&B(T_0)=\frac{\alpha^4}{12\lambda^3}T_0^4\ ,\\
&B(T_c)=0\ ,\quad B(T_+)=-\frac{\alpha^4}{192\lambda^3}T_+^4\ ,
\end{aligned}
\tag{2.15}
$$

where T_b defines the extremum of $B(T)$ [see Eq. (2.17)]. Its derivative is given by

$$
B'(T)=[-\gamma T+\tfrac{1}{3}\alpha v(T)]v^2(T) \tag{2.16}
$$

and has the special values

$$
\begin{aligned}
&B'(0)=\frac{1}{3}\alpha\left[\frac{\gamma}{\lambda}\right]^{3/2}T_0^3\ ,\quad B'(T_b)=0\ ,\\
&T_0B'(T_0)=-\tfrac{9}{8}(3\hat{T}_0^2-1)\hat{T}_0^2L\ ,\\
&-T_cB'(T_c)=\frac{4}{9}\frac{\alpha^2\gamma}{\lambda^2}T_0^2T_c^2=\text{latent heat}\equiv L\ ,\\
&T_+B'(T_+)=\frac{9(3\hat{T}_0^2+1)}{(9\hat{T}_0^2-1)^2}L\ .
\end{aligned}
\tag{2.17}
$$

The graphs of $TB'(T)$ and $B(T)$ are also plotted in Fig. 2. Since $B(T)$ is the difference between the stable and metastable minima, one expects it to increase when T decreases below T_c. However, this happens only until T_b, below which $B(T)$ decreases when $T\to 0$. Again, this unphysical behavior is kept far from the range of metastability if T_0/T_c is not too small.

For the correlation lengths one obtains, in the low-T phase,

$$
\begin{aligned}
\frac{1}{l_l^2}&=V''(v(T),T)\\
&=\frac{\alpha^2}{2\lambda}T^2[1-\tfrac{8}{9}\bar{\lambda}(T)+\sqrt{1-\tfrac{8}{9}\bar{\lambda}(T)}]
\end{aligned}
\tag{2.18}
$$

and, in the high-T phase,

$$
\frac{1}{l_h^2}=M^2(T)=\frac{\alpha^2}{2\lambda}T^2\frac{4}{9}\bar{\lambda}(T)\ ,\quad T_0<T\ . \tag{2.19}
$$

These are also plotted in Fig. 2. At $T=T_c$ both correlation lengths are, as a special property of this quartic parametrization of the effective potential, equal:

$$
\frac{1}{l_h^2(T_c)}=\frac{1}{l_l^2(T_c)}=\frac{\alpha^2}{2\lambda}\frac{4}{9}T_c^2\ . \tag{2.20}
$$

We have thus seen that, in the parametrization (2.2), $v(T)$ and $B(T)$ decrease when T increases from T_0 towards T_c if $T_0>\sqrt{5}/3T_c$ or $T_0>T_c/\sqrt{3}$, respectively. This is what one physically expects: more symmetry for increasing T. The former condition $T_0>0.74T_c$ is stronger and implies

$$
\frac{\alpha^2}{\lambda\gamma}<2\ , \tag{2.21}
$$

which replaces (2.6). Physically, this is the same condition as the usual condition for the validity of the Landau free energy expansion: this is an expansion in the order parameter, which thus should be small compared with its value at $T=0$, which implies that T should not be too far below T_c. Note that for second-order transitions there is also an upper limit: T must not be so close to T_c that fluctuations would lift the system back to the high-T phase. Now these fluctuations back are suppressed by the potential barrier.

B. The equation of state

With the above definitions we can now write down our form for the EOS for EW matter near $T=T_c$:

$$
\begin{aligned}
&p_l(T)=aT^4+B(T)\ ,\quad p_h(T)=aT^4\ ,\\
&s_l(T)=4aT^3+B'(T)\ ,\quad s_h(T)=4aT^3\ ,\\
&\epsilon_l(T)=3aT^4+TB'(T)-B(T)\ ,\quad \epsilon_h(T)=3aT^4\ ,
\end{aligned}
\tag{2.22}
$$

where $a=g_*\pi^2/90$, $g_*=106.75$ for the minimal standard model (SM) (so that $a=11.7$). $B(T)$ is attached with the l phase since both exist only up to $T=T_+$. Note that due to the requirement $B(T_c)=0$ and the equal pressure condition (2.1) we must choose the same a for the two phases in (2.22). This does not mean, without specifying $B(T)$, that particles would be massless in the l phase. Many particles will get their masses at T_c, but provided that $v(T_c)\lesssim T_c$ the masses can be neglected at the phase transition and hence all the relevant effects are within the range of validity of (2.22) collected in $B(T)$. Note also that the mass of the quantum associated with the order parameter is also less than T_c in both phases if $\gamma\lesssim 1$. This EOS cannot be valid for $T\ll T_c$, and for some parameter values s_l may become negative. The least we should require is that $s_l(T_0)>0$, which according to (2.17) implies

$$
\frac{9}{32}(3\hat{T}_0^2-1)\frac{\hat{L}}{a\hat{T}_0^2}=(3\hat{T}_0^2-1)\frac{\alpha^2\gamma}{8a\lambda^2}<1\ .
$$

Thus the range of validity of the EOS increases with decreasing L and increasing number of degrees of freedom $\sim a$.

In view of the complexity of $B(T)$ it is also useful to present an even simpler version based on the approximation

$$
B(T)\approx L\left[1-\frac{T}{T_c}\right]\approx\frac{L}{2}\left[1-\frac{T^2}{T_c^2}\right]\ .
$$

The quadratic form is more convenient since then only T^2 and T^4 appear in p and ϵ. This leads to the EOS

$$
\begin{aligned}
&p_l(T)=aT^4+\frac{L}{2}\left[1-\frac{T^2}{T_c^2}\right]\ ,\quad p_h(T)=aT^4\ ,\\
&s_l(T)=4aT^3-L\frac{T}{T_c^2}\ ,\quad s_h(T)=4aT^3\ ,\\
&\epsilon_l(T)=3aT^4-\frac{L}{2}\left[1+\frac{T^2}{T_c^2}\right]\ ,\quad \epsilon_h(T)=3aT^4\ .
\end{aligned}
\tag{2.23}
$$

The expression for the entropy density of the l phase is positive only for

$$T \geq \left[\frac{L}{4aT_c^4} \right]^{1/2} T_c \ . \tag{2.24}$$

Thus again the domain of validity increases with decreasing L/a. In cosmological applications later the numbers are such that Eq. (2.24) implies $T \gtrsim 0.10 T_c$. This lower limit is also seen in the sound velocity $v_s = dp/d\epsilon$:

$$v_{sl}^2 = \frac{T^2 - L/(4aT_c^2)}{3T^2 - L/(4aT_c^2)} \ , \quad v_{sh}^2 = \tfrac{1}{3} \ .$$

However, one can phenomenologically proceed even one step further and approximate

$$B(T) \approx \frac{L}{4} \left[1 - \frac{T^4}{T_c^4} \right] . \tag{2.25}$$

This leads one directly to the usual bag EOS, used for the quark→hadron phase transition, and conventionally written in the form

$$\begin{aligned} &p_h(T) = a_h T^4 \ , \quad p_q(T) = a_q T^4 - B \ , \\ &s_h(T) = 4a_h T^3 \ , \quad s_q(T) = 4a_q T^3 \ , \\ &\epsilon_h(T) = 3a_h T^4 \ , \quad \epsilon_q(T) = 3a_q T^4 + B \ , \end{aligned} \tag{2.26}$$

where q and h denote the high-T quark and low-T hadron phases, $B = L/4$ is conventionally appended to the q phase, and $a_1 - a_h = B/T_c^4$. Equation (2.26) is, in practice, much simpler than (2.22) and the reason for this is obvious upon comparison of (2.25) with (2.14). The EOS (2.22) can thus also be used to model the quark→hadron transition, but then $B(T)$ has to be determined by some other means [9–12]. Instead of (2.25) one may also use [16–18] an approximation which amounts to replacing B by AT, A = another constant.

C. Parameter values

From our point of view the parameters γ, T_0, α, and λ are phenomenological parameters, to be determined by experiment or observation. In principle, they are derivable from the full microscopic theory. However, one can estimate their magnitudes by using the one-loop finite-T effective potential [15] and the large-T expansions

$$\begin{aligned} V_B &= T \int \frac{d^3k}{(2\pi)^3} \ln(1 - e^{-\sqrt{k^2 + M^2}/T}) \\ &\approx -\frac{\pi^2}{90} T^4 + \frac{M^2}{24} T^2 - \frac{M^3}{12\pi} T \cdots \ , \\ V_F &= -T \int \frac{d^3k}{(2\pi)^3} \ln(1 + e^{-\sqrt{k^2 + M^2}/T}) \\ &\approx -\frac{7\pi^2}{720} T^4 + \frac{M^2}{48} T^2 \cdots \ , \end{aligned} \tag{2.27}$$

where M depends on the mean field ϕ. For the Higgs sector M^2 may be negative and gauge dependent. To get an estimate, we include the Higgs field simply as one scalar field with $M = \sqrt{2\lambda}\phi$. For the minimal standard model one then obtains

$$\begin{aligned} \gamma &= \frac{1}{16} \left[\frac{8}{3}\lambda + 3g^2 + g'^2 + 2g^2 \frac{M_t^2}{M_W^2} \right] , \\ \alpha &= \frac{3}{32\pi} \left[\frac{8}{3} (2\lambda)^{3/2} + 2g^3 + (g^2 + g'^2)^{3/2} \right] . \end{aligned} \tag{2.28}$$

We have above argued that one should not extend the expansion (2.2) down to $T = 0$, it is only valid near $T = T_c$. Thus the coupling λ appearing there need not be the same as the usual zero-temperature four-point self-coupling λ, related to the Higgs-boson mass in the minimal SM by $\lambda = \frac{1}{8} g^2 M_H^2 / M_W^2$. We shall use the rather small number $\lambda = 0.006$, to satisfy the baryon-number retention bound [19], together with (2.28) evaluated for $g = 0.6$, $g' = 0$ and $M_t = M_W$, as reference values:

$$\gamma = 0.1125 \ , \quad \alpha = 0.019\,34 \ , \quad \lambda = 0.006 \ . \tag{2.29}$$

From (2.5) and (2.10) they lead to

$$T_0 = 0.9364 T_c \ , \quad T_+ = 1.0089 T_c$$

and to the combinations

$$\begin{aligned} &\frac{\alpha^2}{\lambda\gamma} = 0.554 \ , \quad \frac{\alpha^2\gamma}{\lambda^2} = 1.17 \ , \quad \frac{\alpha^4}{\lambda^3} = 0.648 \ , \\ &\frac{\alpha}{\lambda^{3/2}} = 41.6 \ , \quad \frac{\alpha^3}{\lambda^{5/2}} = 2.59 \ , \end{aligned} \tag{2.30}$$

relevant for $\hat{T}_0^2$, L, $B(T)$, nucleation probability and surface energy, respectively.

If the extension of (2.2) to $T = 0$ were allowed, one could use the measured value $v(0) = 246$ GeV and Eq. (2.11) to relate the parameters by

$$T_0 = \sqrt{\lambda/\gamma}\, 246 \text{ GeV} \ . \tag{2.31}$$

Although this is not in the spirit of the present approach, it may be of interest to give a set of parameters corresponding to the minimal SM with $M_W = 80.6$ GeV, $M_Z = 91.2$ GeV, $M_t = M_H = 100$ GeV. Then $\lambda = 0.0826$ and from Eq. (2.28), $\alpha = 0.0343$, $\gamma = 0.1844$. From (2.5), (2.10), and (2.31) then $T_0 = 164.6$, $T_c = 166.1$, and $T_+ = 166.3$ GeV. The nucleation analysis of Sec. III with $\alpha/\lambda^{3/2} = 1.45$ will show that the phase transition takes place at $T_f = 166.0$ GeV. However, for this set of parameters the energy of the sphaleron configuration, which is responsible for baryon-number-violating transitions, is found to be $E_{\text{sphaleron}}(T_c)/T_c = 1.56(4\pi/g)(2\alpha/3\lambda) = 8.4$ and not > 45 as required if the ΔB generated is to be retained [19].

III. NUCLEATION PROBABILITY

The formula for the rate of tunneling from the metastable minimum at $\phi = 0$ to the stable minimum at $\phi = v(T)$ (for $T_0 < T < T_c$) contains a dimensionful determinant factor as well as a dimensionless exponential barrier penetration factor [3]:

$$p(t) = p_0 e^{-S(t)} \ . \tag{3.1}$$

The former has not been calculated for the general parametrization (2.2), but one expects it to be of the order of T^4. The barrier factor has been discussed in [3]; here we observe that it can be written in a compact form by expressing it in terms of the function $\bar{\lambda}(T)$ defined in Eq. (2.7).

In general, in this effective theory, $S(t)$ is the extremum of

$$S(t)=\frac{1}{\hbar}\int_0^{\beta\hbar}d\tau\, d^3x\left[\frac{1}{2}\left[\frac{d\phi}{d\tau}\right]^2+\frac{1}{2}(\nabla\phi)^2+V(\phi,T)\right] \tag{3.2}$$

in the space of functions periodic in τ, and with the appropriate boundary conditions. Simple approximations are obtained by considering the large- and small-T limits. In the large-T limit $\beta\hbar\to 0$, $\hbar$ cancels and, scaling the ϕ and x in (2.2) and (3.2) by $\phi=3M^2\psi/2\delta$ and $x=x'/M$, one obtains

$$\begin{aligned}S(t)=\frac{S_3}{T}&=\frac{\alpha}{\lambda^{3/2}}\frac{\sqrt{2\pi}}{3}\bar{\lambda}^{3/2}(T)\\&\quad\times\int_0^\infty d\rho\,\rho^2[(\psi')^2+\psi^2-\psi^3+\tfrac{1}{4}\bar{\lambda}(T)\psi^4]\\&\approx\begin{cases}\dfrac{\alpha}{\lambda^{3/2}}\dfrac{2^{9/2}\pi}{3^5}\dfrac{\bar{\lambda}^{3/2}(T)}{[\bar{\lambda}(T)-1]^2} & \text{SSC},\\ \dfrac{\alpha}{\lambda^{3/2}}4.57\bar{\lambda}^{3/2}(T) & \text{LSC}.\end{cases}\end{aligned} \tag{3.3}$$

Here the two approximations to the large-T approximation are valid in the small supercooling (SSC) ($T_c-T\ll T_c$ when the nucleation takes place) and large supercooling (LSC) (T is somewhere in the middle of the range T_0,T_c) limits. In the SSC limit we also have the result of classical nucleation theory:

$$S_3=\frac{16\pi}{3}\frac{\sigma^3}{[L(1-\hat{T})]^2}, \tag{3.4}$$

where

$$\sigma=\frac{2^{3/2}}{3^4}\frac{\alpha^3}{\lambda^{5/2}}T_c^3 \tag{3.5}$$

is the energy/area of the interface between domains having $\phi=0$ and $\phi=v(T)$. The numerically computed extremal of the integral in (3.3) as well as the two approximations are plotted in Fig. 3.

In the low-T limit one similarly has

$$\begin{aligned}S(t)=S_4&=\frac{\bar{\lambda}(T)\pi^2}{2\lambda}\int_0^\infty d\rho\,\rho^3[(\psi')^2+\psi^2-\psi^3+\tfrac{1}{4}\bar{\lambda}(T)\psi^4]\\&\approx\begin{cases}\dfrac{1}{\lambda}\dfrac{\pi^2}{6}\dfrac{\bar{\lambda}(T)}{[\bar{\lambda}(T)-1]^3} & \text{SSC},\\ \dfrac{1}{\lambda}45.4\bar{\lambda}(T) & \text{LSC}.\end{cases}\end{aligned} \tag{3.6}$$

This is plotted in Fig. 4.

The smaller of S_3/T and S_4 determines the nucleation temperature. Their ratio is plotted in Fig. 5. One sees that S_4 has the best chance of dominating when the system has supercooled at least half way into the metastability range T_0,T_c. Detailed statements can be made only after giving explicit values for the parameters. This holds also for the conditions $S_3/T\gg 1$, $S_4\gg 1$, which must be satisfied for the whole approach to be valid. For reference parameter values (2.29) these conditions demand $\bar{\lambda}(T)\gg 0.03$ for S_3/T and $\bar{\lambda}(T)\gg 0.0001$ for S_4.

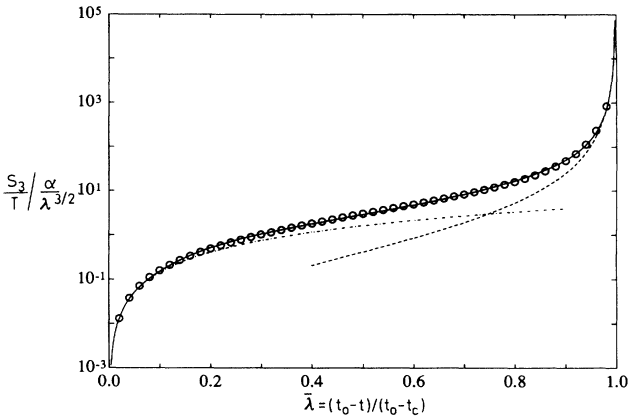

FIG. 3. The high-temperature classical approximation S_3/T to the barrier penetration factor, scaled with $\alpha/\lambda^{3/2}$, together with the two approximations in (3.3). For cosmological EW transition nucleation takes place [Eq. (4.5)] when $S_3/T\approx\ln(M^4_{\text{Planck}}/T_c^4)\approx 160$. For reference parameter values (2.29) $\alpha/\lambda^{3/2}=41.6$ so that nucleation happens at $\bar{\lambda}=(t_0-t)/(t_0-t_c)\approx 0.5$. For the set of parameters after Eq. (2.31) $\alpha/\lambda^{3/2}=1.4$ and at nucleation $\bar{\lambda}\approx 0.93$.

The standard nucleation mechanism of first-order phase transitions is based on the consideration of true extremum bubbles. When the system is cooled towards T_c from above it remains entirely in the h phase even for $T_c<T<T_+$, where the metastable l superheated phase exists. True extremum bubbles start to exist only for $T\le T_c$: for SSC they are of the thin-wall type $[\phi(r)\approx v(T)\theta(r_{\text{crit}}-r)]$ while for LSC they approach Gaussians in r.

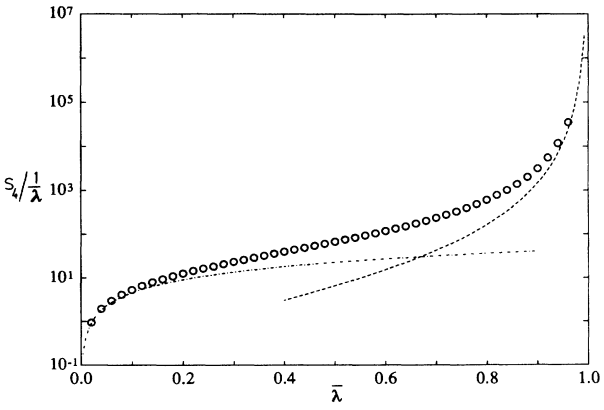

FIG. 4. The small-T O(4)-symmetric approximation S_4 to the barrier penetration factor in Eq. (3.2), scaled with $1/\lambda$, together with the large and small supercooling limits.

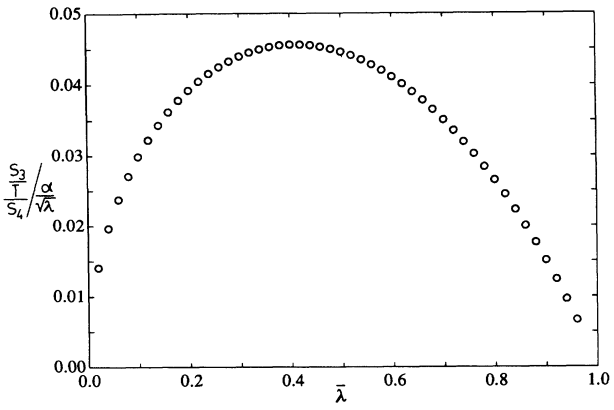

FIG. 5. The ratio $S_3/(TS_4)$, scaled with $\alpha/\sqrt{\bar{\lambda}}$ [=0.25 for reference parameter values (2.29)].

In [14] a modified scenario for the kinetics of first-order transitions is suggested. This is based on the consideration of subcritical bubbles. These bubbles of l phase can be nucleated within the h phase even for $T_c < T < T_+$. If they are nucleated with a sufficiently large probability, the system can be dominantly in the l phase already at T_c and the phase transition is washed out [14]. Our formulation of the problem permits one to work out the kinetics of this scenario rather simply. As in [14] we neglect the shrinking of false-vacuum l bubbles, which conceivably is the main objection to this scenario.

Subcritical bubbles are defined as the configurations

$$\phi_l(r)=v(T)e^{-r^2/l_l^2}, \qquad \phi_h(r)=v(T)(1-e^{-r^2/l_h^2}), \tag{3.7}$$

where the first is a bubble of low-T phase l within high-T phase h and the second vice versa. The bubbles have Gaussian shape, size $\approx$ correlation length of the phase within the bubble, and central strength $\approx v(T)$. For $T_c < T < T_+$ the l phase is only metastable and the $\phi_l(r)$ bubbles disappear rapidly. However, if the rate is large enough, thermal equilibrium between false-vacuum $\phi_l(r)$ and true-vacuum $\phi_h(r)$ bubbles will be established. The rate $\Gamma_h(1/m^3 s)$ of nucleating a bubble (3.7) of l phase in h phase can be estimated by

$$\Gamma_h=\frac{1}{l_h^4}e^{-S_3^h/T}, \tag{3.8}$$

similarly for Γ_l, where, inserting Eq. (3.7) into (3.2) and (3.3),

$$\frac{S_3^h}{T}\equiv\frac{S_3^{l\text{ in }h}}{T}=\frac{\alpha}{\lambda^{3/2}}\frac{3\pi^{3/2}}{16}\frac{(1+z)^{3/2}}{\sqrt{z}}\left[1+\frac{1-z}{6z}-\frac{2^{5/2}}{3^{7/2}z}+\frac{\sqrt{2}(1+z)}{48z}\right], \tag{3.9}$$

$$\frac{S_3^l}{T}=\frac{\alpha}{\lambda^{3/2}}\frac{3\pi^{3/2}}{8\sqrt{2}}\frac{(1+z)^{3/2}}{\sqrt{1-z}}\left\{1+\frac{2^{5/2}}{3}\left[-1+\frac{1}{2^{5/2}}+\left[2-\frac{1}{\sqrt{2}}+\frac{2}{3^{5/2}}\right]\frac{1}{1-z}+\left[-1+\frac{3}{2^{5/2}}-\frac{1}{3^{3/2}}+\frac{1}{32}\right]\frac{1+z}{1-z}\right]\right\}, \tag{3.10}$$

where

$$z\equiv\sqrt{1-\tfrac{8}{9}\bar{\lambda}(T)}\,. \tag{3.11}$$

The two actions (3.9)–(3.10) are equal $=3.030\alpha/\lambda^{3/2}$ for $T=T_c$, $z=\frac{1}{3}$. They are plotted in Fig. 6. Since at the transition temperature the correlation lengths are equal, also the rates at $T=T_c$ satisfy

$$\Gamma_l=\Gamma_h=\frac{4\alpha^4}{81\lambda^2}T_c^4 e^{-3.030\alpha/\lambda^{3/2}}. \tag{3.12}$$

Comparing with the action for true extremals of low-T bubbles in high-T phase in Fig. 3, one observes that the numerical values are similar, about $2.5\alpha/\lambda^{3/2}$, in the middle of the T_0, T_c range. Then the true extremal configurations also resemble the Gaussians in (3.7). Closer to T_c the true extremum action is much larger; the Gaussian configurations (3.7) are not extrema.

Consider now the numbers N_h and N_l of h and l bubbles in some large volume with $N=N_l+N_h=$const. We shall from now on assume that all correlation lengths are $l_h\approx l_l\approx l=1/T_c$. Evidently N_l satisfies the kinetic equation

$$\frac{dN_l}{dt}=V_c(-N_l\Gamma_l+N_h\Gamma_h), \tag{3.13}$$

where $V_c=1/T_c^3$. Thus, in equilibrium,

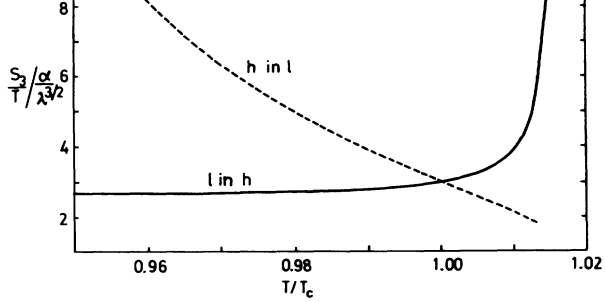

FIG. 6. The actions S_3/T of Eqs. (3.9) and (3.10), scaled by $\alpha/\lambda^{3/2}$, for subcritical bubbles of high-T phase h in low-T phase l (and vice versa). The figure is for $T_0=0.9T_c$, corresponding to $T_+=1.015T_c$.

$$N_l^{\rm eq}(t)=N\frac{\Gamma_h}{\Gamma_h+\Gamma_l}\ .$$

It is simple to write down the general solution of the linear equation (3.13). To see the structure, it is convenient to change into the dimensionless variable $\bar{\lambda}=(t_0-t)/(t_0-t_c)$ defined in Eq. (2.7) and write

$$\frac{dN_l}{d(-\bar{\lambda})}+\frac{t_0-t_c}{l}(e^{S_3^l/T}+e^{S_3^h/T})N_l=\frac{t_0-t_c}{l}Ne^{-S_3^h/T}\ ,$$

where, taking $T_c\sim 100$ GeV and $\hat{T}_0=0.9$,

$$\frac{t_0-t_c}{l}=\frac{0.3M_{\rm Planck}}{\sqrt{g_*}T_c}\left[\frac{1}{\hat{T}_0^2}-1\right]\approx e^{34}\ .$$

Thus

$$\frac{1}{N}\frac{dN_l}{d(-\bar{\lambda})}=e^{34-S_3^h/T}-e^{34-S_3^h/T}(1+e^{-(S_3^l-S_3^h)/T})\frac{N_l}{N}$$

with the initial condition $N_l[\bar{\lambda}(T_+)=\frac{9}{8}]=0$.

Using the numerical value from Eq. (3.12) or Fig. 6 we thus have essentially two cases:

$$\begin{aligned}&\frac{\alpha}{\lambda^{3/2}}\gtrsim\frac{34}{3}\rightarrow N_l(t)=0\ ,\\ &\frac{\alpha}{\lambda^{3/2}}\lesssim\frac{34}{3}\rightarrow N_l(t)=N_l^{eq}(t)\ .\end{aligned}\tag{3.14}$$

In the former case the reaction rate is so small that no appreciable amount of l phase bubbles are nucleated in the stable h phase, in the latter there is an appreciable amount of them and, in particular, at $T=T_c$, $N_l(t_c)=N_h(t_c)$. For the reference parameter values (2.29) $\alpha/\lambda^{3/2}=41.6$ and the reaction rates are by far too small for any equilibrium subcritical bubbles. Hence subcritical bubbles are not very likely to play a dominant role in the EW phase transition. The rates can be large enough for small α, which anyway makes the transition very weakly first order.

Note finally that the entropy density of the l bubbles is smaller than that of the h phase bubbles [Eq. (2.22)]. At T_c, $s_h(T_c)=s_l(T_c)+L/T_c$. If appreciable numbers of l bubbles exist above T_c, entropy conservation will also modify the behavior $R\sim 1/T\sim\sqrt{t}$ of the cosmic scale factor.

IV. SIMULATION OF BUBBLE GROWTH AND COALESCENCE

Bubble nucleation, growth and coalescence has been studied in different contexts earlier [20–21]. Here we present an outline of a Monte Carlo simulation of the event sequence. At time $t>t_c$, $t_cT_c^2\approx 0.3M_{\rm Planck}/\sqrt{g_*}$, the fraction of space still in the unstable high-T phase is

$$h(t)=\exp\left[-\frac{4}{3}\pi v^3\int_{t_c}^{t}dt'p_0e^{-S(t')}(t-t')^3\right]\ ,\tag{4.1}$$

where v is the growth velocity of the bubbles. The initial stages, when v varies with time, are studied in [22]. The exponentiation in (4.1) accounts for the overlap of the bubbles [20].

The integral in (4.1) can be estimated with steepest-descent methods [4–6]. Physically even more transparent is to note [7] that $h(t)$ is so rapidly varying that only values of $S(t')$ near $t'=t$ matter. Expanding $S(t')$ in powers of $t-t'$ one obtains

$$h(t)=\exp\left[-\frac{4}{3}\pi v^3p_0e^{-S(t)}\frac{3!}{[S'(t)]^4}\right]\tag{4.2}$$

provided that

$$-S'(t)(t-t_c)\gg 1\ ,\quad S''(t)\ll 2[S'(t)]^2\ .\tag{4.3}$$

For, say, $S(t)=C/(t-t_c)^p$, where C,p are constants, both conditions are equivalent to $S(t)\gg 1$. For S_3/T the derivative with respect to the scaled time $\bar{\lambda}=(t_0-t)/(t_0-t_c)$ is plotted in Fig. 7.

We are interested in the behavior of $h(t)$ when it approaches 0. Defining t_f by $h(t_f)=1/e$ we obtain, from (4.2),

$$h(t)=\exp(-e^{-S'(t_f)(t-t_f)})\ ,\tag{4.4}$$

where the nucleation time t_f (giving the corresponding nucleation temperature T_f) is determined by solving

$$\frac{4}{3}\pi v^3\frac{3!}{[S'(t_f)]^4}p_0=e^{S(t_f)}\ .\tag{4.5}$$

Numerically, the magnitude of the left-hand side is essentially determined by $t_c^4p_0\approx t_c^4T_c^4\approx(M_{\rm Planck}/T_c)^4\approx 10^{68}$.

Knowing $h(t)$, the fraction of space in which new bubbles can be nucleated and the nucleation rate $p(t)$ we can write the rate of nucleation of bubbles in the form

$$\begin{aligned}\Gamma(t)&=p(t)h(t)=p(t_f)e^{-S'(t_f)(t-t_f)}h(t)\\ &=\frac{p(t_f)}{S'(t_f)}\frac{dh(t)}{dt}\ .\end{aligned}\tag{4.6}$$

The total number of bubbles nucleated by the time t in a volume V then is

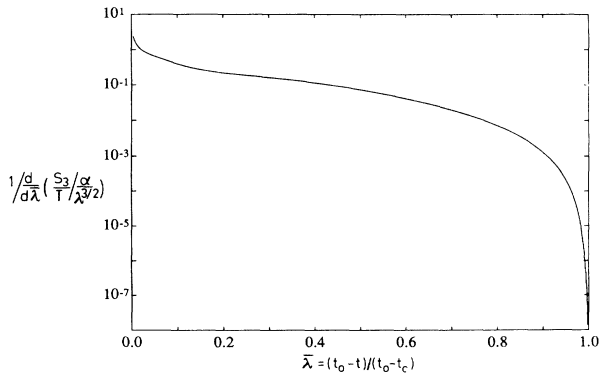

FIG. 7. The inverse of the derivative of S_3/T with respect to $\bar{\lambda}$, scaled with $\alpha/\lambda^{3/2}$. Including the numerical factors from Eq. (4.11) this gives the growth time of bubbles and/or Hubble radius [or from (4.10) the average distance of nucleation centers].

$$N_{\text{bubbles}}(t)=V\int_{t_c}^{t}dt'\Gamma(t')=V\frac{p(t_f)}{-S'(t_f)}[1-h(t)]\ , \quad (4.7)$$

which, using Eq. (4.5), leads to the final density of bubbles:

$$n_{\text{bubbles}}=\frac{p_0}{-S'(t_f)}e^{-S(t_f)}=\frac{[-S'(t_f)]^3}{3!\frac{4}{3}\pi v^3}\ . \quad (4.8)$$

Clearly $R_{\text{nucl}}=n_{\text{bubbles}}^{-1/3}$ defines the average distance of nucleation centers.

The above equations can be analytically solved for the nucleation time t_f (and temperature T_f), the bubble growth time $t_{\text{growth}}=1/[-S'(t_f)]$ and the distance between nucleation centers R_{nucl} in the case (3.4) of classical nucleation and small supercooling. Abbreviating

$$A=\frac{64\pi}{3}\frac{\sigma^3}{L^2T_c}\left[=\frac{2^{13/2}\pi}{3^9}\frac{\alpha^5}{\lambda^{7/2}\gamma^2}\frac{1}{\hat{T}_0^4}=0.24\right], \quad (4.9)$$

where the parentheses refer to the EW case with the reference parameters, one has

$$\begin{aligned}
&S(t)=\frac{A}{(t/t_c-1)^2}\ ,\\
&\frac{t_f}{t_c}=1+\frac{A^{1/2}}{\ln^{1/2}(M_{\text{Planck}}^4/T_c^4)}=1+2\left[1-\frac{T_f}{T_c}\right],\\
&t_{\text{growth}}=\frac{1}{-S'(t_f)}=t_c\frac{\frac{1}{2}A^{1/2}}{\ln^{3/2}(M_{\text{Planck}}^4/T_c^4)}\ ,\\
&R_{\text{nucl}}=(8\pi)^{1/3}v/[-S'(t_f)]\ .
\end{aligned} \quad (4.10)$$

In the general case one has to proceed numerically, first solving t_f from Fig. 3. Then, from the definition (2.7) of $\bar{\lambda}$,

$$\frac{t_c}{t_{\text{growth}}}=\frac{T_0^2}{T_c^2-T_0^2}\frac{\alpha}{\lambda^{3/2}}\left.\frac{dS/(\alpha/\lambda^{3/2})}{d\bar{\lambda}}\right|_{t_f}\ , \quad (4.11)$$

where the derivative is plotted in Fig. 7.

Consider then simulating bubble nucleation and growth in a constant volume V—the expansion of the Universe can be neglected here. The simulation can be based on the fact that the probability that there are no bubbles nucleated in the volume V in the time $t_1<t<t_2$ is

$$p(t_1,t_2)=\exp\left[-\int_{t_1}^{t_2}dt\ Vp(t)\right]\ . \quad (4.12)$$

The simulation can then proceed as follows. (1) Start from some t_1 $(=-\infty)$. (2) Generate a random number $0\le r<1$ and solve t_2 from

$$p(t_1,t_2)=r\ . \quad (4.13)$$

This is the time when the next bubble is nucleated. Writing $\tau=-S'(t_f)t$ the approximate solution of (4.12) is

$$\tau_2=\ln\left[e^{\tau_1}+c_f\ln\frac{1}{4}\right], \quad (4.14)$$

where c_f is a V-dependent constant which can be chosen suitably in the simulation. Note that replacing $\ln r\to\langle\ln r\rangle=-1$ implies $\tau_{n+1}=\ln c_f+\ln(n)$; if $c_f=1/N_{\text{iter}}$, the generation is terminated at $\tau\sim 0$. (3) Choose a random location for the bubble within V. If the location is within an earlier bubble, reject the bubble to be. (4) Increase the radius of all earlier bubbles by $v(t_2-t_1)$. (5) Replace t_1 by t_2 and proceed to 2.

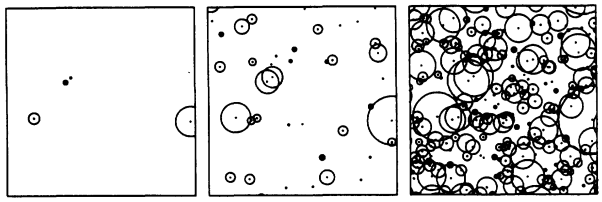

FIG. 8. A two-dimensional simulation of bubble growth. If t_f is defined by area covered by bubbles $=1-1/e$, the three frames of size $(40vt_{\text{growth}})^2$ show the bubble configuration at times $t_f-4.5t_{\text{growth}}$, $t_f-2.5t_{\text{growth}}$, $t_f-0.5t_{\text{growth}}$. Bubble collisions are neglected. To convert to physical units for the QCD phase transition, one can estimate from (4.10) in terms of the Hubble time t_c (taking $\sigma=0.1T_c^3$; $L=10T_c^4$) $t_{\text{growth}}=t_c/180\,000$, $t_c=10\ \mu$s. For the EW phase transition with the reference parameters (2.29), from Figs. 3 and 7, $t_{\text{growth}}=t_{c/360}0$, $t_c=20$ ps.

The result of one simulation is presented in Fig. 8. As far as the conditions (4.3) are satisfied, simulations of all phase transitions irrespective of the degree of supercooling look the same: the physical units of time are given by $t_{\text{growth}}\equiv 1/[-S'(t_f)]$ and of length by vt_{growth}. (See Fig. 9.)

V. COSMIC EXPANSION AND BUBBLE GROWTH AS DEFLAGRATIONS OR DETONATIONS

It is well known that the expanding bubble walls can propagate as deflagrations or detonations. In their analysis the most general problem one can study is what front velocities are allowed by the general conditions of

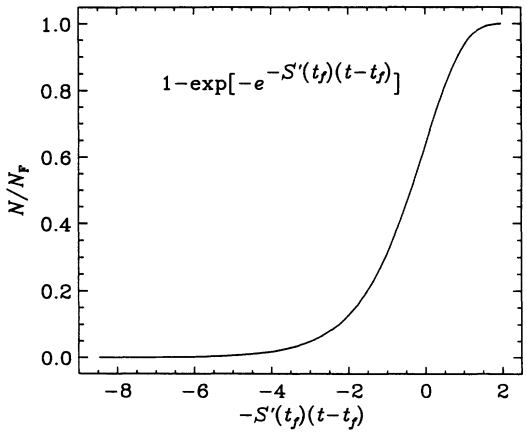

FIG. 9. The number of bubbles N, scaled by the final number $N_F=20\,569$, in a three-dimensional simulation in a volume $(80vt_{\text{growth}})^3$. To this accuracy the result of the simulation and the curve $1-\exp\{-\exp[-S'(t_f)(t-t_f)]\}$ are indistinguishable.

energy-momentum conservation and entropy increase. For the bag EOS (2.26) for QCD matter this analysis has been carried out in [23]. Here we shall do the same for the EOS (2.22) [or (2.23)] for EW matter.

Inserting more information on the interface permits one to make statements on the impossibility of strong deflagrations and rarity of weak detonations [24]. Ultimately one should be able to determine a definite value for the front velocity from microscopic considerations. Here we shall confine ourselves to the general analysis.

An important parameter in a first-order transition is L/ϵ_H, the ratio of the latent heat and the energy density of the high-T phase at T_c. For QCD this is $\lesssim 1$, for the EW theory $\ll 1$. To assess the effects of this difference, it is useful to consider the simplest way of going through a first-order phase transition: one assumes that the transition is infinitely slow and follows the equilibrium EOS with no supercooling. In the cosmological situation the temperature first decreases (Fig. 10) by dilution down to T_c at the Hubble time $t_c = 1/(\sqrt{16\pi a G}\, T_c^2)$. After this the Universe stays at a fixed temperature $T = T_c$ and pressure

$$p_c = p_h(T_c) = p_l(T_c) \tag{5.1}$$

and expands by converting dense h phase to less dense l phase with the energy densities

$$\epsilon_H = \epsilon_h(T_c) = 3aT_c^4 = \epsilon_L + L \equiv \epsilon_l(T_c) + L \ . \tag{5.2}$$

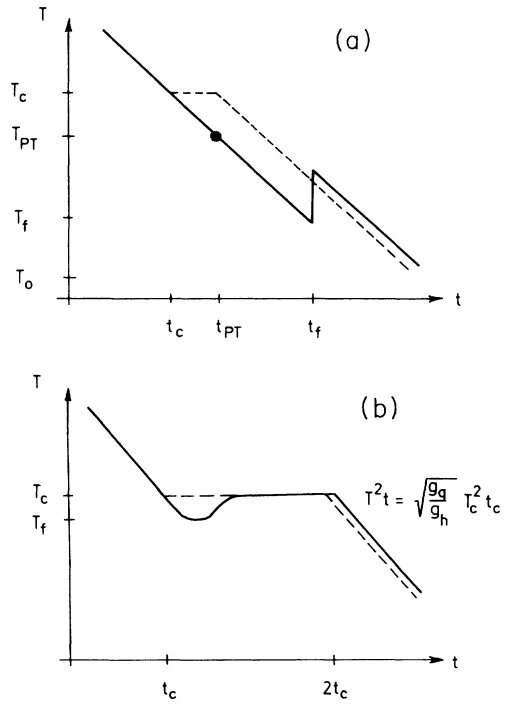

FIG. 10. (a) The schematic behavior of the temperature as a function of time (log-log plot) in the EW phase transition. The dotted line shows the path followed in an equilibrium transition with no supercooling. In practice the transition takes place at T_f with an associated small entropy increase. (b) The same for the quark→hadron transition. After an initial turbulent period the Universe is reheated approximately to T_c.

The time this takes can, from the Einstein equations, be computed to be [25]

$$\frac{t_{PT}-t_c}{t_c} = \frac{4}{3}\left[\frac{\epsilon_H}{p_c}\right]^{1/2}\left[\arctan\left[\frac{\epsilon_H}{p_c}\right]^{1/2} - \arctan\left[\frac{\epsilon_H - L}{p_c}\right]^{1/2}\right]$$

$$\approx \frac{L}{2\epsilon_H} = \frac{2}{27a}\frac{\alpha^2\gamma}{\lambda^2}\frac{T_0^2}{T_c^2} \approx 0.0054 \ , \tag{5.3}$$

where the approximation holds for $L \ll \epsilon_H$, Eq. (2.17) was used for L and the numerical value is for the reference values (2.29), i.e., $\alpha^2\gamma/\lambda^2 = 1.17$, $T_0 = 0.936 T_c$.

An equilibrium transition would thus last for much less than the Hubble time. If the transition did not take place, the Universe would during the time $t_{PT} - t_c$ supercool (Fig. 10) down to the temperature $T_{PT} \approx T_c - T_c L/4\epsilon_H$. This may be very close to the upper end of the metastability range $T_0 < T < T_c$. In view of the earlier nucleation calculations it is quite likely that the nucleation temperature T_f is actually considerably below T_c within the metastability range $T_0 < T < T_c$ [Eq. (4.5)]. For the reference parameter values (2.29) we would have $T_{PT} = 0.9975 T_c$ and $T_f = 0.97 T_c$. Apart from a possible entropy increase associated with the phase transition, the Universe will follow $T \sim 1/R \sim 1/\sqrt{t}$. In particular, the Universe will not go through a period of constant T_c. There may be important supercooling effects and also detonations, which require more supercooling than deflagrations, seem to be possible.

For the quark→hadron phase transition, using the bag EOS (2.26), $a_q/a_h \approx (37+14.25)/(3+14.25) \approx 3$ (14.25 corresponds to inert electron, muon, neutrinos and the photon) and

$$L/\epsilon_Q = (a_q - a_h)/(a_q - \tfrac{1}{4}a_h) \approx 0.73 \ . \tag{5.4}$$

The duration of the equilibrium transition is, from (5.3),

$$\frac{t_{PT}-t_c}{t_c} = \frac{4}{3}\left[\frac{4a_q}{a_h} - 1\right]^{1/2} \times \left[\arctan\left[\frac{4a_q}{a_h} - 1\right]^{1/2} - \arctan\sqrt{3}\right]$$

$$\approx 0.99 \ , \tag{5.5}$$

just about the Hubble time. Now the phase transition would be nucleated at a T_f which is very close to T_c (Fig. 10). The bubbles would grow and fill the Universe with the very dilute hadron phase almost instantaneously. In view of the small amount of supercooling, detonations are hardly possible. However, the Universe has not had time to expand and cannot accommodate this amount of dilute hadron matter—at least not without unrealistic superheating. What happens, instead, is that the shock waves preceding the deflagraton bubbles will reheat the

Universe to T_c and excessive hadron matter production is impeded. Effectively, only small hadron-matter regions with an average distance $R_{\rm nucl}$ [Eq. (4.8)] are formed and the Universe stays for a long time at $T=T_c$ and expands by converting matter from the dense quark phase to the more dilute hadron phase—leptons and the photon are inert.

After this general outline we shall discuss in more detail the phase space available for explosive processes. To do this, go to the rest frame of transition interface, assumed to be planar, and define variables as shown in Fig. 11. Matter in the h phase with $T=T_h$ (which fixes p_h, s_h, and ϵ_h) enters the interface with velocity v_h and matter in the l phase with $T=T_l$ (which fixes p_l, s_l, and ϵ_l) leaves the interface with velocity v_l. A solution of the energy-momentum conservation equations gives

$$v_h v_l=\frac{p_l-p_h}{\epsilon_l-\epsilon_h}\ ,\quad \frac{v_l}{v_h}=\frac{\epsilon_h+p_l}{\epsilon_l+p_h}\ . \tag{5.6}$$

The physically possible values of T_l, T_h are determined by $v_l^2\le 1, v_h^2\le 1$ and by the condition of entropy increase ($\perp$ is the direction perpendicular to the interface)

$$\Delta s_\perp = s_l\gamma_l v_h - s_h\gamma_h v_h \ge 0\ , \tag{5.7}$$

which can be written in the form

$$\frac{s_l}{s_h}\ge\frac{T_l}{T_h}\frac{\epsilon_l+p_h}{\epsilon_h+p_l}\ . \tag{5.8}$$

The solutions can be divided in two classes,

$$\begin{aligned}&\text{deflagrations: } v_l>v_h\ ,\\ &\text{detonations: } v_h>v_l\ ,\end{aligned} \tag{5.9}$$

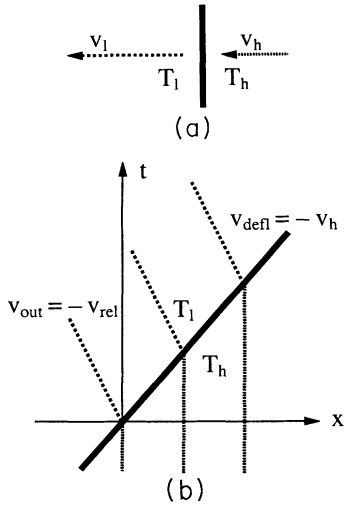

FIG. 11. (a) The variables in the rest frame of the interface. The sole thermodynamic variable T determines p, s, and ϵ for the two phases h and l via the equations of state (2.22)–(2.26). (b) The flow lines for a one-dimensional deflagration.

and a solution with special properties is the one when matter flows out of the interface with sound velocity:

$$\text{Jouguet curve: } v_l=v_{sl}\ .$$

To analyze the possible solutions on the T_h, T_l plane it is useful to plot the curves

$$v_h=v_l=0\ ,\quad v_h=v_l=1\ ,\quad \Delta s_\perp$$

and the Jouguet curve. This can be done analytically for the simplified EW EOS (2.23) (and for the bag EOS (2.25) [23]). The result is

$$\begin{aligned}&v_h=v_l=0\text{: } y^2=x^2+L(1-x)\ ,\\ &v_h=v_l=1\text{: } y^2=x^2-L\ ,\\ &\Delta s_\perp\ge 0\text{: } (x-y)^3+L(x+y+xy-\tfrac{3}{2}x^2-\tfrac{3}{2}y^2)-\tfrac{1}{2}L^2(1-x)\ge 0\ ,\\ &\text{Jouguet: } y^2=x^2-Lx+\tfrac{1}{3}L+\tfrac{1}{6}L^2\pm\frac{2}{\sqrt{3}}[-Lx^3+(2L+L^2)x^2-(2L^2+\tfrac{1}{4}L^3)x+\tfrac{1}{3}L^2+\tfrac{1}{3}L^3+\tfrac{1}{48}L^4]^{1/2}\ ,\end{aligned} \tag{5.10}$$

$$x\equiv\frac{T_l^2}{T_c^2}\ ,\quad y\equiv\frac{T_h^2}{T_c^2}\ ,\quad L\equiv\frac{L}{2p_c}=\frac{L}{2aT_c^4}\ .$$

These curves are plotted in Fig. 12 for $L/2aT_c^4=0.3$. Then the EOS is applicable only for $T>0.38T_c$ [Eq. (2.24)].

The zero entropy change curve always goes through the static interface point $T_h=T_l=T_c$ and in these scenarios the phase transition usually takes place for T close to T_c. It is, therefore, of some interest to give the behavior of the curves (5.10) for small L and to T close to T_c. One finds that

$$\begin{aligned}&v_h=v_l=0\text{: } T_h-1=(1-\tfrac{1}{2}L)(T_c-1)\ ,\\ &v_h=v_l=1\text{: } T_h-1=T_l-1-\tfrac{1}{4}L\ ,\\ &\Delta s_\perp\ge 0\text{: } T_h-1\le-(1-\tfrac{1}{2}L)(T_l-1)\ ,\end{aligned} \tag{5.11}$$

where units are as in (5.10).

The main conclusion from above is that for a small L and large number of degrees of freedom detonations do not require much supercooling. In fact, from (5.11) one finds that detonations are possible for

$$\frac{T_h}{T_c}\le 1-\frac{L}{16aT_c^4}\ . \tag{5.12}$$

For the reference set of parameters this demands initial supercooling only to $T_h=0.9976T_c$ while the phase transition is nucleated for $T_h\approx 0.97T_c$. At these temperatures there is ample phase space for both deflagrations

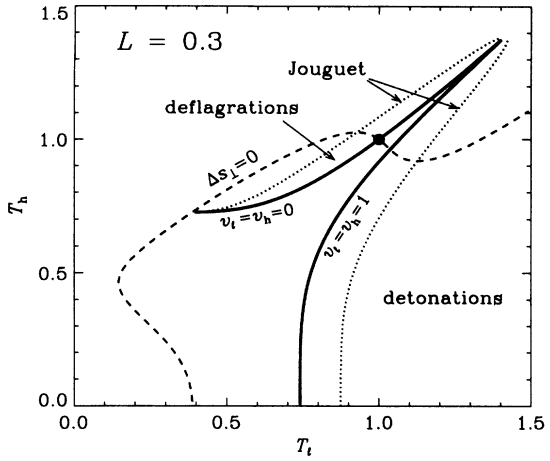

FIG. 12. A plot of the curves (5.10) for $L/2aT_c^4=0.3$. Deflagrations lie below the $\Delta s_\perp=0$ curve (dashed) and above the $v_h=v_l=0$ curve (continuous), detonations lie below the $\Delta s_\perp=0$ curve and to the right of the $v_h=v_l=1$ curve. The dotted curve is the Jouguet curve. The thick point is the point $T_h=T_l=T_c$ corresponding to a stable stationary interface between the two phases.

and detonations.

Consider then the EW EOS (2.22) with full $B(T)$. Since the approximate EOS (2.23) includes terms linear in $T-T_c$ in $B(T)$, differences to the more exact EOS (2.22) appear when values of T further away from T_c become relevant. The first significant effect appearing is T_+, the upper end of the metastable superheated l phase. This is very close to T_c and its existence implies that detonations allowed by the simpler EOS (2.23) actually cannot happen.

Results of a numerical evaluation of Eqs. (5.6)–(5.8) are shown in Figs. 13–17. Figure 13 shows the situation for the reference parameter values (2.29). In addition to the curves discussed above the figure shows curves of

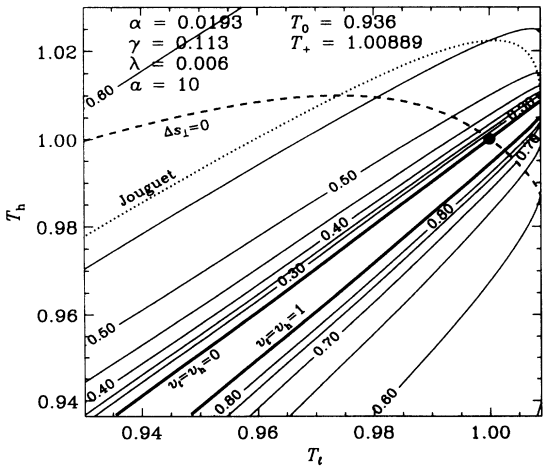

FIG. 13. Curves of constant v_l on the T_l, T_h plane for the values of parameters marked on the figure. The dashed curve is the $\Delta s_\perp=0$ curve, the dotted curve is the $v_l=v_{sl}$ Jouguet curve and the thick point is the static $T_l=T_h=T_c$ point. For $\lambda=0.006$ T_+ is so close to T_c that Jouguet detonations are not possible.

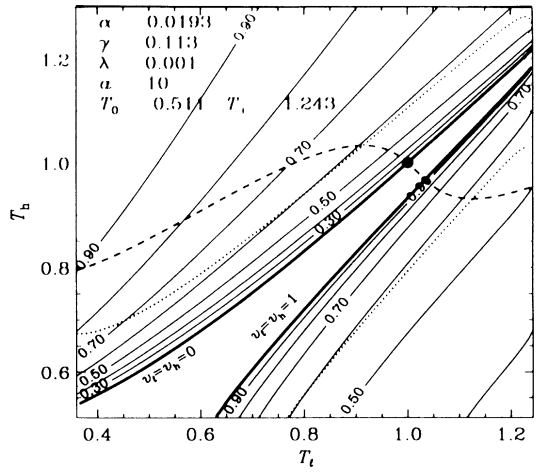

FIG. 14. As Fig. 13 but for $\lambda=0.001$. Now Jouguet detonations are possible.

constant v_l. For these parameter values $T_+=1.008\,89T_c$ is so close to T_c that Jouguet detonations $v_l=v_{sl}$ are not at all possible: they would demand superheating the l phase to temperatures at which this phase no longer exists. Since v_l grows monotonically going to the left from the Jouguet curve, only detonations with $v_l>v_{sl}$ ("weak detonations") are at all possible.

To expose the hydrodynamical effects more clearly we have in Figs. 14–17 decreased λ to 0.001 for which $T_0=0.5113T_c$, $T_+=1.243T_c$, and $L/(2aT_c^4)=0.2087$. Curves of constant v_l, v_h, and $v_{\rm rel}$ are shown in Figs. 14–16. Note how the special role played by the Jouguet curve is clearly seen in Fig. 15: at fixed T_h, v_h has a maximum (minimum) for deflagrations (detonations) along the Jouguet curve.

The amount of entropy created in the interface per unit area and time is shown in Fig. 17 on the T_l, T_h plane. It varies mildly from deflagrations but blows up for detonations approaching the $v_h=v_l=1$ line. For deflagrations

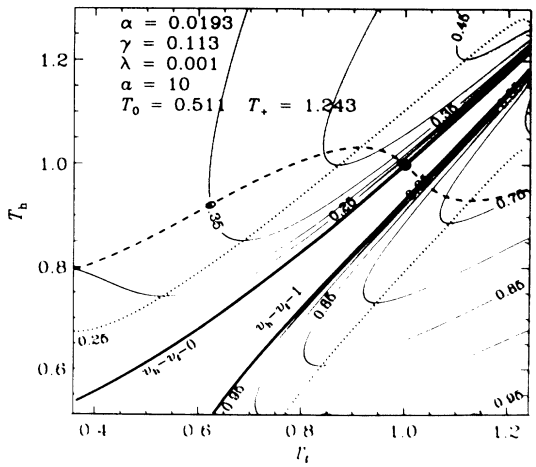

FIG. 15. As Fig. 14 but for curves of constant v_h, which is also the velocity of the deflagration or detonation front propagating into h matter at rest at temperature T_h.

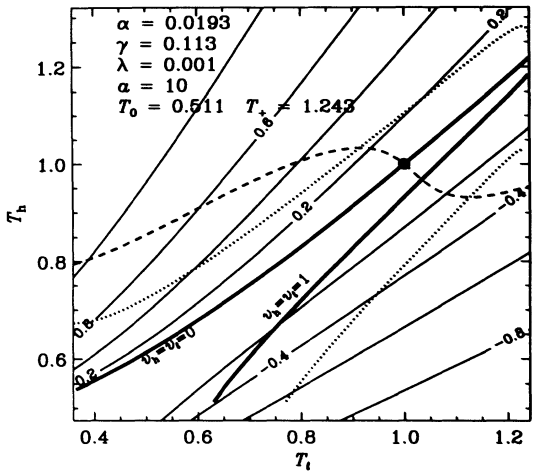

FIG. 16. As Fig. 14 but for curves of constant $v_{\rm rel}$ which is also the velocity of the l matter ejected by a deflagration or detonation front propagating into h matter at rest at temperature T_h. The change in sign implies that a deflagration ejects the matter in a direction opposite to the front itself [Fig. 11(b)], a detonation to the same direction.

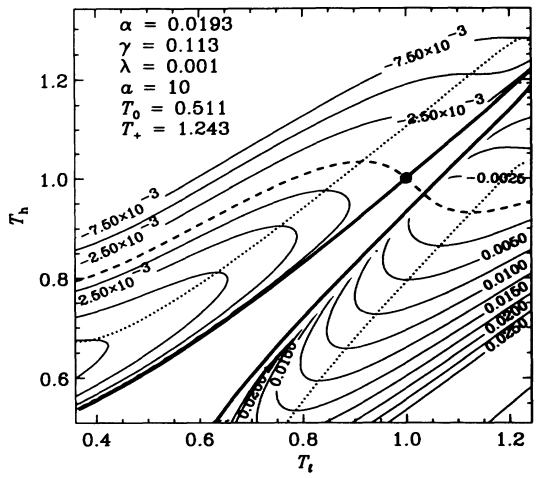

FIG. 17. As Fig. 14 but for curves of constant entropy flux $\Delta s_\perp$ through the interface, in units of T_c^3 (or $1/m^2 s$).

entropy production is maximal (at fixed T_h and varying T_l) along the Jouguet curve, for detonations it is minimal.

The results of this section show that, from the point of view of general conservation rules and for reasonable parameters for the cosmological EW phase transition, there is ample phase space for the phase transition proceeding either as a deflagration or detonation. One interesting detail is that the closeness of the upper limit T_+ of the metastable superheated branch of the l phase to T_c may reduce the phase space available for detonations and leave only weak detonations. To clarify what happens in these cases one should follow the acceleration of the walls of the initially nucleated bubble using the numerical methods of [22].

If one inserts some information on the structure of the interface [24] one can conclude that processes in which the velocity of the matter in the new l phase, flowing out of the interface, is larger than the sound velocity, $v_l > v_{sl}$, are impossible. Deflagrations of this type (strong deflagrations) never occur; detonations of this type can happen under special conditions. The elimination of strong deflagrations leaves a weak deflagration with a single microscopically determined velocity as a possible solution. In view of the above remarks on the effects of T_+ detonations may be completely eliminated as a possible mechanism.

VI. CONCLUSIONS

We have in this paper studied the kinetics of first-order phase transitions using as the starting point a Landau-Ginzburg-type mean-field expansion of the free energy density of the system. The expansion depends on three dimensionless parameters γ, α, and λ and on temperature T_0, the lowest temperature of existence of the high-temperature phase h. These parameters fix the coexistence temperature T_c and the highest temperature of existence T_+ of the low-temperature phase l. The expansion is valid for T near T_c, and the coefficients, although they may also be approximated by the one-loop form of the finite-T effective potential, are in principle phenomenological coefficients to be determined from experiment or observation.

For equilibrium phenomena the mean-field expansion gives rise to an equation of state of the form $p_l(T)=aT^4+B(T)$, $p_h(T)=aT^4$. We studied the behavior of $B(T)$, $B'(T)$, and $v(T)$, the value of the order parameter in the l phase, in detail. It is interesting to note that also the corresponding quark→hadron phase transition in QCD can be modeled with a similar EOS, only $B(T)$ then has to be determined by different means [9–12,26].

For kinetic phenomena the exponential barrier factors can be computed in terms of the potential and we showed that, although the potential depends on four parameters, the tunneling action is essentially a function of one variable only, the scaled time $\bar{\lambda}(T)=(t_0-t)/(t_0-t_c)$, $t_0T_0^2=t_cT_c^2$. Bubble nucleation and growth was simulated and the distance between nucleation centers computed, also as a function of $\bar{\lambda}$.

The simulation of bubble growth left the growth velocity open. We studied what velocities are possible assuming only the general constraints of energy-momentum conservation and entropy increase. Because T_+ may be very close to T_c, the low-T phase cannot sustain much superheating and corresponding detonations, strong detonations, may be excluded. Since weak detonations can appear only under very special circumstances, it may be that the entire detonation family of explosive processes is eliminated. The phase transition will then proceed as a weak deflagration with a single microscopically determinable velocity.

ACKNOWLEDGMENTS

We thank the Academy of Finland, the Finnish Cultural Foundation and the Magnus Ehrnrooth Foundation for financial support. K.K. thanks Larry McLerran for discussions and TPI, Minneapolis for hospitality.

[1] V. A. Kuzmin, V. A. Rubakov, and M. E. Shaposhnikov, Phys. Lett. **155B**, 36 (1985).
[2] L. McLerran, M. Shaposhnikov, M. Turok, and M. Voloshin, Phys. Lett. B **256**, 451 (1991).
[3] A. D. Linde, Nucl. Phys. **B126**, 421 (1983).
[4] C. J. Hogan, Phys. Lett. **133B**, 172 (1983).
[5] T. DeGrand and K. Kajantie, Phys. Lett. **147B**, 273 (1984).
[6] K. Kajantie and H. Kurki-Suonio, Phys. Rev. D **34**, 1719 (1986).
[7] G. Fuller, G. Mathews, and C. Alcock, Phys. Rev. D **37**, 1380 (1988).
[8] J. H. Applegate, C. J. Hogan, and R. J. Scherrer, Phys. Rev. D **35**, 1151 (1987).
[9] J. Kapusta, Nucl. Phys. **B190**, 425 (1981).
[10] B. Müller and J. Rafelski, Phys. Lett. **101B**, 111 (1981).
[11] M. Ninomiya and N. Sakai, Nucl. Phys. **B190**, 316 (1981).
[12] A. Cabo, O. K. Kalashnikov, and A. E. Shabad, Nucl. Phys. **B185**, 473 (1981).
[13] F. Y. Wu, Rev. Mod. Phys. **54**, 235 (1982).
[14] M. Gleiser, E. Kolb, and R. Watkins, Nucl. Phys. **B364**, 411 (1991).
[15] L. Dolan and R. Jackiw, Phys. Rev. D **9**, 3320 (1974).
[16] C.-G. Källman, Phys. Lett. **134B**, 363 (1984).
[17] S. A. Bonometto and L. Sokolowski, Phys. Lett. **107A**, 210 (1985).
[18] M. I. Gorenstein and O. A. Mogilevsky, Z. Phys. C **38**, 161 (1988).
[19] A. I. Bochkarev, S. V. Kuzmin, and M. E. Shaposhnikov, Phys. Rev. D **43**, 369 (1991).
[20] A. Guth and E. Weinberg, Phys. Rev. D **23**, 876 (1981).
[21] B. Meyer, C. Alcock, G. Mathews, and G. Fuller, Phys. Rev. D **43**, 1079 (1991).
[22] J. C. Miller and O. Pantano, Phys. Rev. D **40**, 1789 (1989); **42**, 3334 (1990).
[23] M. Gyulassy, K. Kajantie, H. Kurki-Suonio, and L. McLerran, Nucl. Phys. **B237**, 477 (1984).
[24] R. Courant and K. O. Friedrichs, *Supersonic Flow and Shock Waves* (Springer-Verlag, New York, 1976).
[25] E. Suhonen, Phys. Lett. **119B**, 81 (1982).
[26] B. A. Campbell, John Ellis, and K. A. Olive, Phys. Lett. B **235**, 325 (1990).